

Symbol-Aware Reasoning with Masked Discrete Diffusion for Handwritten Mathematical Expression Recognition

Takaya Kawakatsu
 Preferred Networks, Inc.
 1-6-1 Otemachi, Chiyoda, Tokyo, Japan.
 kat.nii.ac.jp@gmail.com

Ryo Ishiyama
 Kyushu University
 Fukuoka, Japan.
 ryo.ishiyama@human.ait.kyushu-u.ac.jp

Abstract

Handwritten Mathematical Expression Recognition (HMER) requires reasoning over diverse symbols and 2D structural layouts, yet autoregressive models struggle with exposure bias and syntactic inconsistency. We present a discrete diffusion framework that reformulates HMER as iterative symbolic refinement instead of sequential generation. Through multi-step remasking, the proposal progressively refines both symbols and structural relations, removing causal dependencies and improving structural consistency. A symbol-aware tokenization and Random-Masking Mutual Learning further enhance syntactic alignment and robustness to handwriting diversity. On the MathWriting benchmark, the proposal achieves 5.56% CER and 60.42% EM, outperforming strong Transformer and commercial baselines. Consistent gains on CROHME 2014–2023 demonstrate that discrete diffusion provides a new paradigm for structure-aware visual recognition beyond generative modeling.

1. Introduction

Handwritten Mathematical Expression Recognition (HMER) aims to interpret visual mathematical symbols and convert them into structured markup such as \LaTeX . Unlike standard Optical Character Recognition (OCR), HMER is more challenging due to two types of ambiguity: (1) *visual ambiguity*, caused by diverse handwriting styles and symbol shapes; and (2) *syntactic ambiguity*, arising from complex two-dimensional layouts such as superscripts, subscripts, fractions, and radicals. For example, a cursive “z” may resemble “2”, and $(a + b)/c$ can be misread as $a + (b/c)$ if hierarchical syntax is not properly inferred. HMER thus requires both fine-grained visual perception and globally consistent structural reasoning.

Despite advances in sequence-to-sequence models, maintaining structural coherence remains difficult. Most

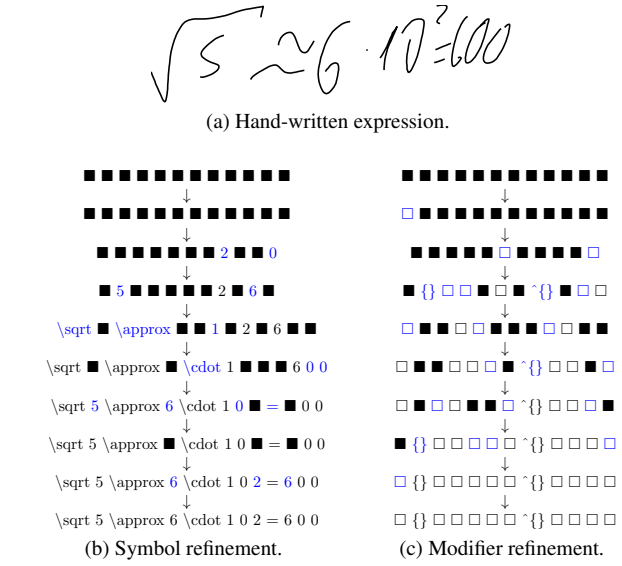


Figure 1. Illustration of the symbolic reasoning process in the proposal. (a) Handwritten expression. (b) Symbol refinement. (c) Modifier refinement. Starting from a fully masked sequence, the proposal iteratively unmasks and re-masks tokens through discrete diffusion to jointly recover symbols and structural relations.

prior approaches [23–26] adopt an autoregressive (AR) encoder–decoder framework, which generates \LaTeX tokens sequentially but suffers from *exposure bias*, where early prediction errors propagate through the sequence. In complex formulas, attention mechanisms often fail to align visual and structural cues, leading to over- or under-parsing. Because \LaTeX syntax distributes dependencies across multiple interrelated tokens, even a single mistake can cascade and is difficult to correct locally.

To overcome these limitations, syntax-aware models [5, 8, 19, 26] encode syntax trees or graph relations for grammatical consistency, while non-autoregressive (NAR) models [11] mitigate exposure bias via parallel generation. However, syntax-aware models often lack flexibility, and

NAR models—though faster—struggle to refine ambiguous or partially incorrect structures. An ideal framework should therefore unify *structural consistency*, *stability*, and *robustness to ambiguity*.

We introduce a discrete diffusion framework that reformulates HMER as an *iterative symbolic refinement* process. Instead of generating tokens sequentially, the proposal starts from a fully masked sequence and iteratively remasks and unmasks it to reconstruct the correct expression. This formulation removes causal dependencies inherent in AR decoding while enabling gradual refinement of both symbols and structural relations—capabilities beyond standard NAR models.

To enhance structural alignment, we propose a *symbol-aware tokenization* scheme that decomposes expressions into visible symbols and structural modifiers in one-to-one correspondence (Fig. 1). This representation preserves syntactic integrity while simplifying grammatical dependencies, allowing local refinements without breaking global structure. We also introduce *Random-Masking Mutual Learning (RMML)*, which enforces consistency across masking conditions by minimizing the KL divergence [7] between differently masked views, improving robustness to handwriting variation and structural ambiguity.

Comprehensive experiments demonstrate that the proposal achieves state-of-the-art performance. On the MathWriting [4] benchmark, it attains a Character Error Rate (CER) of 5.56% and an Exact Match (EM) accuracy of 60.42%, outperforming Google OCR and CoMER. On CROHME 2014–2023 [12, 14, 15, 18], the proposal further improves EM accuracy by up to 4.2 points. These results confirm that discrete diffusion enables robust and consistent structural reasoning, establishing a new paradigm for non-generative recognition tasks.

Contributions.

- Reformulate HMER as a discrete diffusion process, enabling iterative symbolic refinement without exposure bias.
- Design a symbol-aware tokenization scheme that preserves syntactic consistency while reducing representational complexity.
- Integrate Random-Masking Mutual Learning to improve robustness to handwriting diversity and structural ambiguity.
- Empirically validate the proposal on MathWriting and CROHME, achieving state-of-the-art accuracy and improved structural stability.

2. Methodology

Our approach departs fundamentally from autoregressive (AR) architectures. Instead of sequentially generating \LaTeX tokens, we formulate handwritten mathematical expression recognition as an *iterative remasking* process within a dis-

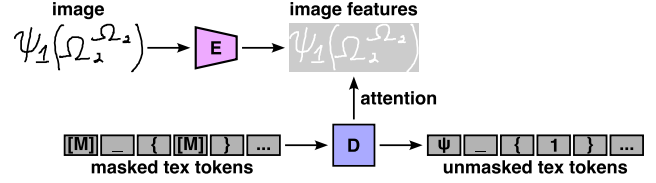


Figure 2. Overall architecture of the proposal. The framework comprises a Vision Transformer (ViT) image encoder and a formula decoder. The encoder extracts visual features from a 224×224 handwritten expression image, while the decoder iteratively refines masked \LaTeX tokens through discrete diffusion to reconstruct the complete expression.

Algorithm 1 Forward (re-)masking process

```

1: Input: Token sequence  $x_0$  and time  $t$ 
2: for  $i = 1 \dots M$  do
3:   Sample  $u_i \sim \mathcal{U}(0, 1)$ 
4:   if  $u_i < t/T$  then
5:      $x_{t,i} \leftarrow \text{MASK}$ 
6:   else
7:      $x_{t,i} \leftarrow x_{0,i}$ 
8:   end if
9: end for
10: Output: Masked sequence  $x_t$ 

```

crete diffusion framework. Each expression starts as a fully masked token sequence, and at each diffusion step the model predicts and replaces masked tokens to progressively reconstruct the complete expression. This parallel refinement removes causal dependencies, mitigating exposure bias while preserving global structural consistency and enabling efficient inference. Fig. 2 shows the architecture.

2.1. Problem Definition

Given a token sequence x of length M , we define a discrete diffusion process [16] that alternates between masking (forward) Alg. 1 and unmasking (reverse) Alg. 2 steps. In this formulation, the forward process progressively increases the masking ratio until all tokens are hidden (x_T), while the reverse process iteratively predicts and refines tokens through a sequence of remasking operations. This discrete diffusion formulation eliminates causal dependencies inherent to autoregressive decoding and enables gradual symbolic refinement while maintaining global structural consistency.

2.2. Symbol-Aware Tokenization

The discrete diffusion process enables iterative refinement rather than left-to-right generation, yet directly applying diffusion to raw \LaTeX sequences leads to structural inconsistencies. In \LaTeX , even a simple structural modification (e.g., converting $x2$ to $\{x\}^{\{2\}}$) requires multiple de-

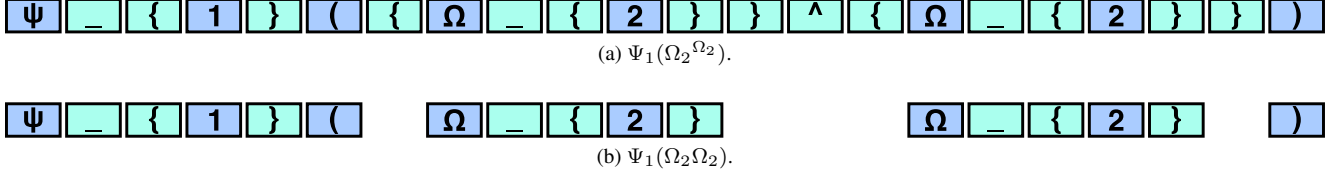


Figure 3. Example of structural editing in a \LaTeX token sequence. When removing a superscript (e.g., converting x^2 to $x2$), multiple dependent tokens must be deleted and subsequent token positions shift forward, altering positional encodings. This demonstrates that directly applying diffusion to raw \LaTeX sequences can easily break syntactic consistency, motivating the need for a symbol-level formulation.

Algorithm 2 Reverse unmasking process

```

1: Initialize:  $x_T \leftarrow [\text{MASK}, \dots, \text{MASK}]$ 
2: for  $t = T, \dots, 1$  do
3:    $x_{t-1} \leftarrow \text{Remask}(\arg \max p(x_{t-1}|x_t), t)$ 
4: end for
5: Output: Expression  $x_0$ 

```

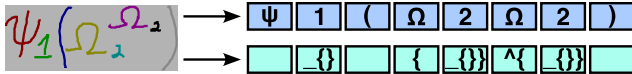


Figure 4. Illustration of symbol-aware tokenization. A \LaTeX expression is decomposed into visible symbols and structural modifiers (e.g., braces, superscripts, subscripts), which are aligned on a one-to-one basis. By integrating modifier embeddings into the corresponding symbols, the model forms a unified symbol-level representation that preserves syntactic consistency while simplifying grammar. This representation shortens sequence length and stabilizes diffusion-based reconstruction.

pendent tokens, such as braces and superscript markers as shown in Fig. 3. These discontinuous edits violate the local token-wise denoising assumption and hinder syntactic stability.

To address this problem, we propose a *symbol-aware tokenization* (SAT) as shown in Fig. 4 that decomposes an expression into visible symbols and invisible structural modifiers. Symbols correspond to observable handwritten symbols (e.g., digits, variables, operators), while modifiers encode spatial and syntactic relations such as superscripts, subscripts, and grouping parentheses.

All modifiers are first removed from the \LaTeX sequence. Then, the removed modifiers are analyzed and aligned to their corresponding visible symbols, forming per-symbol *modifier embeddings*. For instance, in $\{x\}^{\{2\}}$, visible tokens are x and 2 , while the braces and superscript modifier are assigned to their respective symbols. Each visible token thus pairs with a modifier embedding, yielding aligned token-structure pairs of equal length.

The final representation is obtained by summing the symbol and modifier embeddings, integrating visual and syntactic information into a unified token representation. This symbol-level representation shortens sequence length,

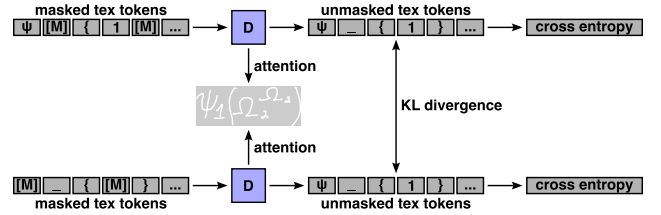


Figure 5. Overview of Random-Masking Mutual Learning (RMML). Two randomly masked variants of the same formula are reconstructed through a shared diffusion decoder, and their predicted token distributions are aligned via KL-divergence regularization to enhance robustness to handwriting and structural variations.

improves Transformer attention efficiency, and allows local structural edits without breaking global consistency.

2.3. Random-Masking Mutual Learning

Ambiguity in handwritten expressions arises from two major factors: (1) *symbol-level ambiguity*, caused by visually similar characters, and (2) *structure-level ambiguity*, due to variations in layout or writing scale. These ambiguities are dynamic, context-dependent, and writer-specific. For instance, a curved “2” may resemble “Z” or “γ”, and a small superscript may enhance structural clarity but reduce legibility.

To enhance generalization under such variability, we introduce *Random-Masking Mutual Learning (RMML)*, extending deep mutual learning [22] to the discrete diffusion setting as shown in Fig. 5. In standard diffusion training, an expression is reconstructed from a masked sequence via iterative denoising. RMML augments this by generating two independently masked variants of the same formula, F_1 and F_2 , with different random masking patterns.

Both masked inputs are denoised by the same decoder, which predicts token distributions for each view. We enforce consistency between the two distributions by minimizing the Kullback–Leibler (KL) divergence [7]:

$$\mathcal{L}_{\text{KL}} = D_{\text{KL}}(P_{F_1} \| P_{F_2}) + D_{\text{KL}}(P_{F_2} \| P_{F_1}). \quad (1)$$

The overall objective combines this term with the standard

cross-entropy loss:

$$\mathcal{L} = \mathcal{L}_{\text{CE}} + \mathcal{L}_{\text{KL}}. \quad (2)$$

3. Related Work

Offline handwritten mathematical expression recognition (HMER) aims to convert handwritten mathematical symbols into structured markup languages such as \LaTeX . Unlike standard text OCR, HMER requires understanding two-dimensional spatial layouts and hierarchical relations among symbols such as superscripts, subscripts, fractions, and radicals. The CROHME benchmark series [12, 14, 15, 18] has played a central role in standardizing this task, providing datasets (2014, 2016, 2019, 2023) that remain the de facto benchmarks for academic comparison.

Research on HMER has evolved through three major stages: (1) a transition from rule-based to deep sequence-to-sequence models, (2) the emergence of syntax-aware decoders, and (3) recent expansions toward large-scale learning, NAR inference, and multimodal reasoning. We summarize each direction below.

3.1. Sequence-to-Sequence Models

Following the success of attention-based encoder-decoder frameworks, HMER has been widely formulated as an image-to-markup translation problem. Transformer-based BTTR [24] achieved bidirectional training within a single decoder, improving the balance of contextual dependencies. Attention Aggregation with Bi-directional Mutual Learning [6] introduced two complementary decoders operating in opposite directions and performing mutual knowledge distillation to capture both local and global contexts. CoMER [23] incorporated an explicit coverage modeling module to mitigate over-parsing and under-parsing errors. General Category Network (GCN) [21] jointly predicted coarse-grained symbol categories (digits, operators, relations, etc.), reducing visual confusions. ICAL [25] introduced implicit character-aided learning, predicting unobserved structural markers to strengthen contextual reasoning and syntax recovery. These advances improved token-level accuracy but still suffered from exposure bias due to left-to-right decoding.

3.2. Syntax-Aware Models

Because mathematical expressions inherently form hierarchical trees, several works have explored structure-aware decoding. Tree-Structured Decoder [20] first generated hierarchical trees directly instead of linear token sequences, achieving strong generalization on deeply nested expressions. TDv2 [17] removed fixed traversal order constraints for more flexible tree generation. Syntax-Aware Network [19] embedded grammar rules and syntax-tree guidance to reduce structural errors, while Counting-Aware Network [8] introduced a symbol-counting auxiliary task to

prevent token omissions and duplications. TAMER [26] introduced a Tree-Aware Transformer that jointly evaluates structural validity during decoding, while PosFormer [5] proposed a Position Forest representation with implicit attention correction, explicitly encoding spatial and hierarchical relations. Although these models enforce grammatical consistency, they often trade off flexibility and inference efficiency.

3.3. Large-Scale Data and Pretraining

Data scarcity has long been a bottleneck for HMER. Tex80M [9] constructed a synthetic dataset of 80 million augmented \LaTeX expressions, revealing clear scaling laws between dataset size and recognition accuracy. MathWriting [4] further released 230k real handwritten samples and 400k synthetic online expressions, providing a large unified benchmark for robust training and evaluation. Such large-scale resources have enabled more generalizable models and paved the way for diffusion-based and multimodal approaches.

3.4. Non-Autoregressive and Diffusion Models

For inference efficiency, NAMER [11] proposed the first NAR framework for HMER, consisting of a visual-aware tokenizer and a parallel graph decoder that jointly predict tokens and relations, achieving $6\text{--}7\times$ faster inference. While these methods alleviate exposure bias, they lack the ability to iteratively refine ambiguous structures. Our work builds on this direction by introducing a discrete diffusion process that enables iterative symbolic reconstruction and structural consistency beyond one-shot NAR decoding.

3.5. Multi-Modal and Vision-Language Models

Recent studies integrate vision and language modeling to further improve generalization. Uni-MuMER [10] fine-tuned large vision-language models under a unified multitask objective, while MMHMER [3] explored multi-view and multi-task fusion for handwritten expression recognition. These approaches demonstrate the potential of multimodal pretraining; however, they still rely on AR decoding and do not explicitly address structural ambiguity. In contrast, the proposal employs diffusion-based symbolic reasoning to unify visual and syntactic refinement in a non-generative recognition setting.

4. Experiments

We conduct extensive experiments to evaluate the effectiveness of the proposal on standard handwritten mathematical expression recognition benchmarks.

4.1. Datasets

We evaluate the proposal on two standard benchmarks for handwritten mathematical expression recognition: **Math**-

Writing and **CROHME**. Both datasets are provided in InkML format, containing stroke coordinate sequences (X–Y time series) with corresponding \LaTeX annotations.

4.1.1. MathWriting

MathWriting [4] contains 230K human-written and 400K synthetic samples. Handwritten data are split into training, validation, and test sets, while synthetic data are generated by fitting handwritten-style symbols into bounding boxes of compiled \LaTeX formulas. The 90th percentile of formula length in synthetic data is 68 tokens (vs. 51 tokens median in human data), indicating higher structural complexity and improved generalization when included. Following the original paper, we use all 626K samples (real + synthetic) for training.

Each stroke sequence is rasterized into a 224×224 binary image with 1-pixel line width, normalized for consistent scaling. The dataset provides standardized \LaTeX labels, allowing evaluation using Character Error Rate (CER). No data augmentation is applied in our experiments to ensure fair comparison.

4.1.2. CROHME

The CROHME benchmark [12, 14, 15] remains the most widely used testbed for HMER. We use the 2014, 2016, 2019, and 2023 editions for evaluation. Each sample includes handwritten strokes and a \LaTeX label, but annotations are not standardized. CROHME itself does not provide rasterized images.

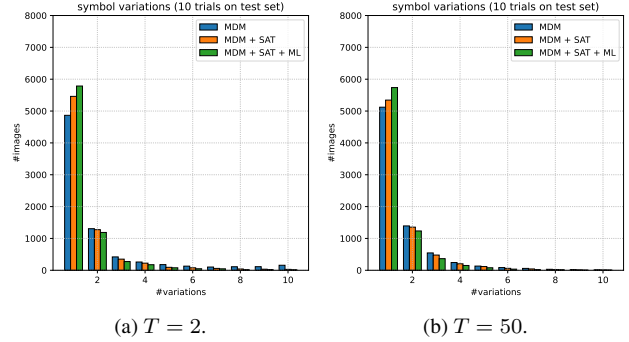
To ensure consistency, we rescale all CROHME samples to a fixed resolution of 224×224 and rasterize them with a 1-pixel stroke width. Unlike our setting, most prior works [23–26] were trained and evaluated on individually rescaled images, but the official CROHME toolkit does not define or justify such instance-specific scaling. The official guideline [12] provides a rendering script that uniformly rescales all expressions to the same pixel resolution, and we strictly follow this procedure to guarantee reproducibility. This normalization often results in lower absolute accuracy than reimplementations using variable scaling, but it ensures fair and reproducible evaluation.

Given that the CROHME training set is relatively small, we use MathWriting for training and treat CROHME purely as a held-out evaluation set. This cross-dataset setup eliminates confounding factors from scale or normalization differences, enabling fair comparison under identical training conditions.

4.2. Metrics

4.2.1. MathWriting

Following the original MathWriting protocol [4], we evaluate recognition performance using *Character Error Rate* (CER) and *Exact Match* (EM). CER is defined as the total number of incorrect tokens divided by the total number of



(a) $T = 2$. (b) $T = 50$.

Figure 6. Output diversity analysis of the masked diffusion model (MDM). Each ablation model performs 10 independent decoding trials for the same handwritten expression, and the number of distinct outputs is counted. Subfigures (a) and (b) show diversity in the symbol sequence with $T = 2$ and $T = 50$, respectively. Both *symbol-aware tokenization (SAT)* and *mutual learning (ML)* effectively suppress excessive output variability while maintaining recognition accuracy, leading to more stable predictions.

tokens across all test samples. EM measures the proportion of expressions that exactly match the ground-truth \LaTeX label. In addition, we report the proportions of expressions that differ by at most one or two tokens from the reference, providing a more fine-grained view of near-correct predictions. Unlike CROHME, the MathWriting paper does not mention the use of `LgEval` [13]; since the dataset already applies strong normalization of token order, we perform purely text-based evaluation. For ablation studies, we further measure the *Syntax Error Rate* (SER), defined as the proportion of decoded expressions in which the number of opening and closing braces ('{' and '}') does not match.

4.2.2. CROHME

For the CROHME benchmarks [12, 14, 15, 18], we follow the official competition protocol and evaluate performance using *Exact Match* (EM) with the `LgEval` [13] toolkit. Unlike simple text matching, `LgEval` performs graph-based structural evaluation that recognizes equivalent expressions even when token order differs, yielding a more accurate measure of mathematical correctness. This procedure constitutes the standard and legitimate evaluation protocol for CROHME.

4.3. Comparison with SOTA Models

Table 1 and Table 2 summarize quantitative comparisons on the MathWriting and CROHME benchmarks. All results are reported in percentage without data augmentation.

Table 1 contains both *offline* and *online* handwritten mathematical expression recognition models. Offline recognition takes rasterized images of expressions as input, while online recognition operates directly on the pen trajectory sequences (X–Y–T coordinates). Hybrid models such as

Table 1. Comparison of recognition performance on the **MathWriting** benchmark. We report Character Error Rate (CER, \downarrow) and Exact Match accuracy (EM, \uparrow) for existing models and our proposed method. \dagger indicates our reimplementations under the same training setup. “Stroke” input denotes online recognition based on sequential pen trajectories (X–Y–T), whereas “Image” corresponds to offline recognition from rasterized expressions. Results for *Proposal* are averaged over 10 runs. *Proposal* applies the Symbol-Aware Tokenization (SAT) only, whereas *ProposalML* further incorporates Random-Masking Mutual Learning (RMML). Previous results are from [4].

Method	Inputs				Valid split				Test split			
	Image	Stroke	FPS	Param	CER \downarrow	EM \uparrow	$\leq 1 \uparrow$	$\leq 2 \uparrow$	CER \downarrow	EM \uparrow	$\leq 1 \uparrow$	$\leq 2 \uparrow$
CTC	-	✓	-	35M	4.52	71.00	81.00	-	5.49	60.00	72.00	-
PaLI	✓	✓	-	700M	4.47	76.00	83.00	-	5.95	64.00	73.00	-
PaLIGemma	✓	✓	-	3B	3.95	80.00	86.00	-	5.97	69.00	77.00	-
Google OCR	✓	-	-	-	6.50	64.00	76.00	-	7.17	53.00	68.00	-
BTTR \dagger	✓	-	1.77	6M	6.45	60.42	72.02	76.41	6.85	53.36	65.53	70.94
CoMER \dagger	✓	-	1.62	6M	5.96	61.23	72.41	76.64	6.50	54.53	65.65	71.31
ICAL \dagger	✓	-	1.68	7M	5.43	63.44	74.49	78.67	6.03	57.68	68.17	73.67
Proposal	✓	-	0.62	28M	4.77	70.59	84.89	90.69	5.56	60.42	78.00	86.28
ProposalML	✓	-	0.62	28M	4.70	70.64	84.83	90.75	5.55	59.60	77.94	86.04

Table 2. Comparison of recognition accuracy on the CROHME 2014–2019 benchmarks. We report Exact Match (EM, \uparrow) in percentage for existing models and our method. \dagger denotes our reimplementations under a unified setting, where all CROHME samples are rescaled to 224×224 resolution. Original works rendered CROHME data at variable resolutions, while our fixed-resolution setup ensures fair and reproducible evaluation. All methods are trained without data augmentation, and *Proposal* results are averaged over 10 runs. Previous results are from [8, 19, 20, 23–26].

Method	Resolution	Training	CROHME 2014			CROHME 2016			CROHME 2019		
			EM \uparrow	$\leq 1 \uparrow$	$\leq 2 \uparrow$	EM \uparrow	$\leq 1 \uparrow$	$\leq 2 \uparrow$	EM \uparrow	$\leq 1 \uparrow$	$\leq 2 \uparrow$
WAP	Variable	CROHME	46.55	61.16	65.21	44.55	57.10	61.55	-	-	-
CAN-DWAP	Variable	CROHME	57.00	74.21	80.61	56.06	71.49	79.51	54.88	71.98	79.40
CAN-ABM	Variable	CROHME	57.26	74.52	82.03	56.15	72.71	80.30	55.96	72.73	80.57
DWAP-TD	Variable	CROHME	49.10	64.20	67.80	48.50	62.30	65.30	51.40	66.10	69.10
SAN	Variable	CROHME	56.20	72.60	79.20	53.60	69.60	76.80	53.50	69.30	70.10
BTTR	Variable	CROHME	53.96	66.02	70.28	52.31	63.90	68.61	52.96	65.97	69.14
CoMER	Variable	CROHME	59.33	71.70	75.66	59.81	74.37	80.30	62.97	77.40	81.40
ICAL	Variable	CROHME	60.63	75.99	82.80	58.79	76.06	83.38	60.51	78.00	84.63
TAMER	Variable	CROHME	61.23	76.77	83.25	60.26	76.91	84.05	61.97	78.97	85.80
BTTR \dagger	224 \times 224	MathWriting	57.71	67.75	71.50	52.66	63.56	68.70	54.30	64.47	68.06
CoMER \dagger	224 \times 224	MathWriting	60.24	69.07	72.41	56.06	65.13	69.83	58.05	67.06	71.06
ICAL \dagger	224 \times 224	MathWriting	62.37	71.20	74.54	59.02	69.14	73.06	60.97	69.39	73.39
Proposal	224 \times 224	MathWriting	63.23	73.31	78.62	63.23	75.08	80.46	60.66	73.60	79.14

PaLI [2] and PaLIGemma [1] leverage both modalities and large-scale multimodal pretraining. For clarity, we distinguish these categories in the discussion below.

4.3.1. Offline models

Among image-based offline recognizers, the proposal achieves a Character Error Rate (CER) of 4.77% on the validation set and 5.56% on the test set, improving upon

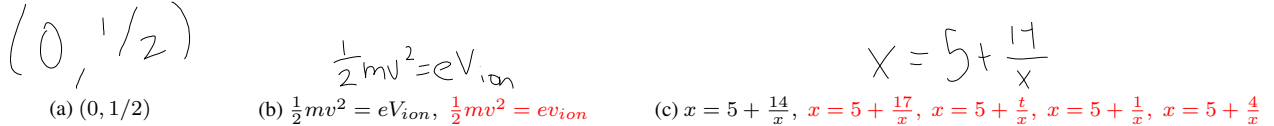


Figure 7. Case study of output diversity in *Proposal*. Each cell shows an input handwritten expression (left) and the decoded results produced from ten independent diffusion runs. Correct predictions are shown in black, while incorrect ones are highlighted in red. Expressions that are visually clear and unambiguous yield identical outputs across all trials, whereas ambiguous or poorly written expressions produce multiple plausible parses.

Table 3. Comparison of recognition accuracy on the **CROHME 2023** benchmark. We report Exact Match (EM, \uparrow) in percentage. \dagger indicates our reimplementation under the same training and pre-processing setup as CROHME 2014–2019. All models are trained on **MathWriting** and evaluated on CROHME 2023 without data augmentation. Results for *Proposal* are averaged over 10 runs.

CROHME 2023					
Method	EM \uparrow	$\leq 1 \uparrow$	$\leq 2 \uparrow$	$\leq 3 \uparrow$	$\leq 4 \uparrow$
BTTR \dagger	53.65	63.96	68.00	69.96	71.35
CoMER \dagger	56.91	66.39	69.87	71.52	73.04
ICAL \dagger	58.30	67.39	71.35	73.04	74.74
Proposal	60.78	74.28	80.42	83.87	86.40

the strongest Transformer-based baseline (ICAL, 6.03%) by 0.47 absolute points and outperforming Google OCR by 1.61 points. In EM accuracy, the proposal attains 70.59% (valid) and 60.42% (test), which are 2.7–6.6 points higher than prior image-based recognizers. These gains are achieved without any external pretraining or auxiliary handwriting data, confirming the effectiveness of the discrete diffusion formulation in improving structural consistency and robustness.

4.3.2. Online and hybrid models

Online HMER systems, which directly exploit stroke-level temporal information, generally achieve substantially higher accuracy than offline approaches. As noted in the MathWriting paper [4], even a simple CTC-based sequence model outperforms Google OCR, demonstrating that the online modality inherently provides stronger cues about writing order and symbol segmentation. PaLI and PaLIGemma are large-scale vision–language models that combine both image and stroke inputs, benefiting from multimodal representations and pretraining on hundreds of millions of examples. While PaLIGemma achieves higher overall accuracy on MathWriting than our offline recognizer, its advantage primarily stems from access to richer modalities and massive pretraining resources. In contrast, the proposal operates purely in the offline setting without large-scale multimodal training, yet achieves partially com-

petitive performance that approaches multimodal VLMs. This comparison highlights the efficiency and adaptability of our discrete diffusion framework in learning symbolic structure even from limited 2D visual input.

4.3.3. CROHME benchmarks

On **CROHME** 2014–2019, the proposal also achieves the best overall accuracy among models trained under the same resolution setting (224×224). Specifically, it records EM of 63.23%, 63.23%, and 60.66% on CROHME 2014, 2016, and 2019, respectively—surpassing the reimplemented ICAL baseline by up to 4.21 points. To further verify cross-year generalization, we additionally evaluate the proposal on the **CROHME 2023** benchmark. Under the same unified preprocessing and resolution (224×224 px), the proposal achieves an EM of 60.78%, outperforming the reimplemented *CoMER* and *ICAL* baselines by 3.9 and 2.5 points, respectively. These consistent improvements across four CROHME editions (2014–2023) reinforce that the discrete diffusion framework provides stable structural reasoning and robustness to style variation, even when trained exclusively on MathWriting.

For reproducibility, we reimplemented three representative Transformer-based baselines—BTTR, CoMER, and ICAL—under identical training and preprocessing settings.

4.4. Ablation Study

We analyze the contribution of each proposed component in Table 4. The evaluation is conducted on MathWriting under varying diffusion steps $T = \{2, 10, 50\}$.

The *symbol-aware tokenization (SAT)* reduces CER and SER by 0.7 and 3 points respectively compared to the baseline on the validation set for $T = 2$, confirming its effectiveness in enforcing syntactic consistency. As diffusion steps increase, both CER and SER gradually improve and converge around $T = 50$, which is therefore adopted as the default configuration in all main experiments. Adding *Random-Masking Mutual Learning (ML)* further decreases CER to 4.70% and SER to 0.93%, demonstrating enhanced robustness under varying masking conditions.

At larger diffusion steps ($T = 50$), the relative gains from SAT and ML become smaller, as the iterative refinement itself stabilizes the decoding process. However, for shallower diffusion schedules ($T \leq 10$), both components

Table 4. Ablation and efficiency analysis on the **MathWriting** dataset. We evaluate the impact of *Symbol-Aware Tokenization (SAT)* and *Random-Masking Mutual Learning (ML)* under different diffusion step counts ($T = 2, 10, 50$). Metrics include Character Error Rate (CER, \downarrow), Exact Match (EM, \uparrow), and Syntax Error Rate (SER, \downarrow). Both SAT and ML consistently reduce CER and SER while improving EM; combining them yields the best overall accuracy. Increasing diffusion steps leads to gradual improvement, with performance converging around $T = 50$, which is used as the default setting in all main experiments.

(a) Valid set.														
SAT	ML	FPS			CER \downarrow			EM \uparrow			SER \downarrow			
		2	10	50	2	10	50	2	10	50	2	10	50	
-	-	4.20	2.12	0.62	6.18	4.99	4.84	66.63	69.42	69.92	6.24	1.77	1.08	
✓	-	4.45	2.20	0.62	5.48	4.87	4.77	67.78	70.17	70.59	3.21	1.46	1.13	
✓	✓	4.43	2.19	0.62	5.33	4.77	4.70	68.46	70.22	70.64	2.60	1.19	0.93	

(b) Test set.														
SAT	ML	FPS			CER \downarrow			EM \uparrow			SER \downarrow			
		2	10	50	2	10	50	2	10	50	2	10	50	
-	-	4.30	2.10	0.61	7.32	5.91	5.76	54.32	58.27	58.99	8.81	2.72	1.74	
✓	-	4.44	2.19	0.62	6.41	5.69	5.56	56.36	59.53	60.42	5.02	2.21	1.67	
✓	✓	4.40	2.18	0.62	6.18	5.65	5.55	56.39	58.89	59.60	4.34	2.10	1.66	

yield notably larger improvements in CER and SER, indicating that they are particularly effective when fewer refinement iterations are allowed. Since $T = 10$ or smaller achieves more than 2 FPS in inference speed, these configurations offer a practical trade-off between accuracy and efficiency for latency-sensitive applications.

4.5. Output Diversity

While diffusion models inherently introduce stochasticity, excessive output variation may indicate instability. To evaluate this, we measure output diversity by performing 10 independent decoding runs per input. Fig. 6 counts distinct visible symbol sequences. The baseline model exhibits larger diversity, whereas both SAT and ML suppress unnecessary variability, producing more deterministic and consistent outputs.

Fig. 7 provides qualitative examples of this behavior. For clear and unambiguous handwritten expressions, all ten decoding trials yield identical results, indicating convergence to a single valid parse. In contrast, ambiguous or poorly written expressions produce multiple plausible structures. Interestingly, some of the alternative outputs, though labeled incorrect, remain mathematically valid—showing that the proposal can explore syntactically consistent alternatives under uncertainty, rather than collapsing to arbitrary noise.

5. Conclusion

We introduced a discrete diffusion framework that reformulates handwritten mathematical expression recognition as an iterative symbolic refinement process. By progressively unmasking and remasking tokens, it removes exposure bias and improves global structural consistency. A *symbol-aware tokenization* and *Random-Masking Mutual Learning* further enhance syntactic alignment and robustness.

Experiments on the MathWriting and CROHME benchmarks show that the proposal achieves state-of-the-art performance, reducing CER to 5.56% and improving EM to 60.42%, while yielding superior structural stability and consistency. These results establish discrete diffusion as a promising paradigm for structure-aware recognition beyond generative modeling. Future work will explore faster inference and extensions to online and multimodal handwritten understanding.

References

- [1] Lucas Beyer, Andreas Steiner, André Susano Pinto, Alexander Kolesnikov, Xiao Wang, Daniel Salz, Maxim Neumann, Ibrahim Alabdulmohsin, Michael Tschannen, Emanuele Bugliarello, Thomas Unterthiner, Daniel Keysers, Skanda Koppula, Fangyu Liu, Adam Grycner, Alexey Gritsenko, Neil Houlsby, Manoj Kumar, Keran Rong, Julian Eisenschlos, Rishabh Kabra, Matthias Bauer, Matko Bošnjak, Xi Chen, Matthias Minderer, Paul Voigtlaender, Ioana Bica, Ivana Balazevic, Joan Puigcerver, Pinelopi Papalampidi,

Olivier Henaff, Xi Xiong, Radu Soricut, Jeremiah Harmsen, and Xiaohua Zhai. PaliGemma: A versatile 3b VLM for transfer. 2024. 6

[2] Xi Chen, Xiao Wang, Soravit Changpinyo, AJ Piergiovanni, Piotr Padlewski, Daniel Salz, Sebastian Goodman, Adam Grycner, Basil Mustafa, Lucas Beyer, Alexander Kolesnikov, Joan Puigcerver, Nan Ding, Keran Rong, Hassan Akbari, Gaurav Mishra, Linting Xue, Ashish V. Thapliyal, James Bradbury, Weicheng Kuo, Mojtaba Seyedhosseini, Chao Jia, Burcu Karagol Ayan, Carlos Riquelme, Andreas Steiner, Anelia Angelova, Xiaohua Zhai, Neil Houlsby, and Radu Soricut. PaLI: A jointly-scaled multilingual language-image model. In *International Conference on Learning Representations (ICLR)*, 2023. 6

[3] Ziyu Chen, Feng Yang, Rui Wang, and Haoyi Zhao. MMH-MER: Multi-viewer and multi-task for handwritten mathematical expression recognition. 2025. 4

[4] Philippe Gervais, Anastasiia Fadeeva, and Andrii Maksai. MathWriting: A dataset for handwritten mathematical expression recognition. In *ACM SIGKDD Conference on Knowledge Discovery and Data Mining*, pages 5459–5469, 2025. 2, 4, 5, 6, 7

[5] Tongkun Guan, Chengyu Lin, Wei Shen, and Xiaokang Yang. PosFormer: Recognizing complex handwritten mathematical expression with position forest transformer. In *Computer Vision – ECCV*, pages 130–147, 2025. 1, 4

[6] Xiaoxiang Han, Qiaohong Liu, Ziqi Han, Yuanjie Lin, and Naiyue Xu. Handwritten mathematical expression recognition via GCattention-based encoder and bidirectional mutual learning transformer. In *Chinese Conference on Pattern Recognition and Computer Vision*, pages 282–294, 2022. 4

[7] Solomon Kullback and Richard A. Leibler. On information and sufficiency. *The Annals of Mathematical Statistics*, 22(1), 1951. 2, 3

[8] Bohan Li, Ye Yuan, Dingkang Liang, Xiao Liu, Zhilong Ji, Jinfeng Bai, Wenyu Liu, and Xiang Bai. When counting meets hmer: Counting-aware network for handwritten mathematical expression recognition. In *Computer Vision – ECCV*, pages 197–214, 2022. 1, 4, 6

[9] Haoyang Li, Jiaqing Li, Jialun Cao, Zongyuan Yang, and Yongping Xiong. Towards scalable training for handwritten mathematical expression recognition. 2024. 4

[10] Yu Li, Jin Jiang, Jianhua Zhu, Shuai Peng, Baole Wei, Yuxuan Zhou, and Liangcai Gao. Uni-MuMER: Unified multi-task fine-tuning of vision-language model for handwritten mathematical expression recognition. *NeurIPS*, 2025. 4

[11] Chenyu Liu, Jia Pan, Jinshui Hu, Baocai Yin, Bing Yin, Mingjun Chen, Cong Liu, Jun Du, and Qingfeng Liu. NAMER: Non-autoregressive modeling for handwritten mathematical expression recognition. In *Computer Vision – ECCV*, pages 273–291, 2025. 1, 4

[12] Mahshad Mahdavi, Richard Zanibbi, Harold Mouchere, Christian Viard-Gaudin, and Utpal Garain. ICDAR 2019 CROHME + TFD: Competition on recognition of handwritten mathematical expressions and typeset formula detection. In *International Conference on Document Analysis and Recognition (ICDAR)*, pages 1533–1538, 2019. 2, 4, 5

[13] Harold Mouchère, Christian Viard-Gaudin, Richard Zanibbi, Utpal Garain, Dae Hwan Kim, and Jin Hyung Kim. ICDAR 2013 CROHME: Third international competition on recognition of online handwritten mathematical expressions. In *International Conference on Document Analysis and Recognition (ICDAR)*, pages 14280–1432, 2013. 5

[14] Harold Mouchère, Christian Viard-Gaudin, Richard Zanibbi, and Utpal Garain. ICFHR 2014 competition on recognition of on-line handwritten mathematical expressions (CROHME 2014). In *International Conference on Frontiers in Handwriting Recognition*, pages 791–796, 2014. 2, 4, 5

[15] Harold Mouchère, Christian Viard-Gaudin, Richard Zanibbi, and Utpal Garain. ICFHR2016 CROHME: Competition on recognition of online handwritten mathematical expressions. In *International Conference on Frontiers in Handwriting Recognition (ICFHR)*, pages 607–612, 2016. 2, 4, 5

[16] Subham Sekhar Sahoo, Marianne Arriola, Aaron Gokaslan, Edgar Mariano Marroquin, Alexander M Rush, Yair Schiff, Justin T Chiu, and Volodymyr Kuleshov. Simple and effective masked diffusion language models. In *Advances in Neural Information Processing Systems (NeurIPS)*, pages 130136–130184, 2024. 2

[17] Changjie Wu, Jun Du, Yunqing Li, Jianshu Zhang, Chen Yang, Bo Ren, and Yiqing Hu. TDv2: A novel tree-structured decoder for offline mathematical expression recognition. In *AAAI Conference on Artificial Intelligence*, pages 2694–2702, 2022. 4

[18] Yeqing Xie, Harold Mouchère, Foteini Simitsira Liliwicki, Sumit Rakesh, Rajkumar Saini, Masaki Nakagawa, Cuong Tuan Nguyen, and Thanh-Nghia Truong. ICDAR 2023 CROHME: Competition on recognition of handwritten mathematical expressions. In *Document Analysis and Recognition - ICDAR*, pages 553–565, 2023. 2, 4, 5

[19] Ye Yuan, Xiao Liu, Wondimu Dikubab, Hui Liu, Zhilong Ji, Zhongqin Wu, and Xiang Bai. Syntax-aware network for handwritten mathematical expression recognition. In *IEEE/CVF Conference on Computer Vision and Pattern Recognition (CVPR)*, pages 4543–4552, 2022. 1, 4, 6

[20] Jianshu Zhang, Jun Du, Yongxin Yang, Yi-Zhe Song, Si Wei, and Lirong Dai. A tree-structured decoder for image-to-markup generation. In *International Conference on Machine Learning*, pages 11076–11085, 2020. 4, 6

[21] Xinyu Zhang, Han Ying, Ye Tao, Youlu Xing, and Guihuan Feng. General category network: Handwritten mathematical expression recognition with coarse-grained recognition task. In *IEEE International Conference on Acoustics, Speech and Signal Processing (ICASSP)*, pages 1–5, 2023. 4

[22] Ying Zhang, Tao Xiang, Timothy M. Hospedales, and Huchuan Lu. Deep mutual learning. In *IEEE/CVF Conference on Computer Vision and Pattern Recognition (CVPR)*, pages 4320–4328, 2018. 3

[23] Wenqi Zhao and Liangcai Gao. CoMER: Modeling coverage for transformer-based handwritten mathematical expression recognition. In *Computer Vision – ECCV*, pages 392–408, 2022. 1, 4, 5, 6

[24] Wenqi Zhao, Liangcai Gao, Zuoyu Yan, Shuai Peng, Lin Du, and Ziyin Zhang. Handwritten mathematical expression

recognition with bidirectionally trained transformer. In *Document Analysis and Recognition – ICDAR*, pages 570–584, 2021. 4

[25] Jianhua Zhu, Liangcai Gao, and Wenqi Zhao. ICAL: Implicit character-aided learning for enhanced handwritten mathematical expression recognition. In *Document Analysis and Recognition – ICDAR*, pages 21–37, 2024. 4

[26] Jianhua Zhu, Wenqi Zhao, Yu Li, Xingjian Hu, and Liangcai Gao. TAMER: Tree-aware transformer for handwritten mathematical expression recognition. In *AAAI Conference on Artificial Intelligence*, pages 10950–10958, 2025. 1, 4, 5, 6